

Possibility of a continuous phase transition in random-anisotropy magnets with a generic random-axis distribution

D. Shapoval^{1,2}, M. Dudka^{1,2,3}, A.A. Fedorenko⁴, and Yu. Holovatch^{1,2,5}

¹*Institute for Condensed Matter Physics, National Academy of Sciences of Ukraine, 1 Sviatsitskii Street, UA-79011 Lviv, Ukraine*

²*L⁴ Collaboration & Doctoral College for the Statistical Physics of Complex Systems, Leipzig-Lorraine-Lviv-Coventry, Europe*

³*Institute of Theoretical Physics, Faculty of Physics, University of Warsaw, Pasteura 5, 02-093 Warsaw, Poland*

⁴*Université de Lyon, ENS de Lyon, Université Claude Bernard, CNRS, Laboratoire de Physique, F-69342 Lyon, France*

⁵*Centre for Fluid and Complex Systems, Coventry University, Coventry, CV1 5FB, United Kingdom*

We reconsider the problem of the critical behavior of a three-dimensional $O(m)$ symmetric magnetic system in the presence of random anisotropy disorder with a generic trimodal random axis distribution. By introducing n replicas to average over disorder it can be coarse-grained to a ϕ^4 -theory with $m \times n$ component order parameter and five coupling constants taken in the limit of $n \rightarrow 0$. Using a field theory approach we renormalize the model to two-loop order and calculate the β -functions within the ε expansion and directly in three dimensions. We analyze the corresponding renormalization group flows with the help of the Padé-Borel resummation technique. We show that there is no stable fixed point accessible from physical initial conditions whose existence was argued in the previous studies. This may indicate an absence of a long-range ordered phase in the presence of random anisotropy disorder with a generic random axis distribution.

I INTRODUCTION

The structural disorder is inevitably present in many magnetic systems which undergo a phase transition. Of particular interest is its impact near the critical points, where even weak disorder can drastically modify the scaling behavior.^{1–3} One can classify different types of disorder according to the symmetry it breaks. The most common types of disorder include: (i) random bond/site disorder where randomness couples linearly to the local energy density, and thus, can be viewed as local critical temperature fluctuations⁴; (ii) random field disorder where the order parameter is linearly coupled to a random symmetry breaking field⁵; and (iii) random anisotropy disorder in systems with continuous symmetry where the coupling of the order parameter to disorder is bilinear⁶.

The effect of quenched⁷ random bond/site disorder on the critical behavior of magnetic systems has been studied for several decades and is now relatively well understood. In particular according to the Harris criterion⁸ it modifies the critical behavior of a d -dimensional system if the correlation length exponent ν of the pure system satisfies the inequality $\nu < 2/d$. The corresponding critical exponents have been computed by renormalization group (RG) methods using $\varepsilon = 4 - d$ expansion up to four-loop order⁹, directly in three dimensions up to six-loop order¹⁰ and using a non-perturbative approach.¹¹

The Harris criterion can be generalized to the random bond/site disorder correlated in space as a power law $\sim 1/r^a$ which is proven to be relevant for $\nu < \max(2/a, 2/d)$.¹² The corresponding critical exponents have been computed using double expansion in $\varepsilon = 4 - d$ and $\delta = 4 - a$,^{12–15} directly in three dimensions,^{16,17} in two dimensions using a mapping to Dirac fermions¹⁸ and numerical simulations.^{19,20} Another model with anisotropic correlated disorder in which extended defects are strongly correlated in ε_d dimensions and randomly distributed over the remaining $d - \varepsilon_d$ dimensions was pro-

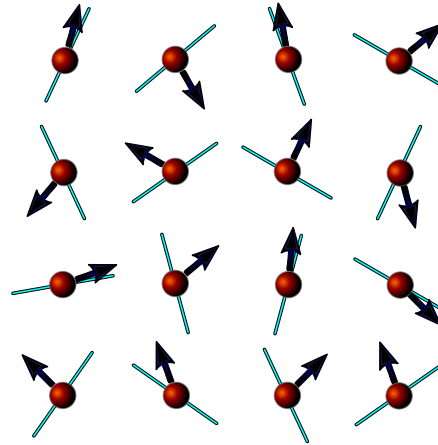


FIG. 1. Sketch plot of the two-dimensional RAM. Red discs depict sites of the lattice with spins (black arrows) on them. Random local anisotropy axis direction on each site is shown by light blue line.

posed in Ref. 21 and studied in Refs. 22–31.

The impact of quenched random fields and random anisotropies is usually more profound and much less studied. For instance, a complete understanding of the simplest model, the random field Ising model (RFIM), is still lacking despite significant numerical and analytical efforts³². It has been shown that the standard perturbative RG calculations lead to incorrect results due to the so-called dimensional reduction³³. The only known way to overcome this obstacle for the RFIM is the non-perturbative RG developed in Refs. 34 and 35, which however, is a sophisticated and hardly controllable method (see also recent review Ref. 36). For systems

with continuous symmetry the isotropically distributed random fields and random anisotropies drive the low critical dimension of $O(m)$ symmetric systems from $d_l = 2$ to $d_l = 4$ with a new quasi-long-range order (QLRO) emerging below d_l^{37} . Both the QLRO below d_l and the ferromagnetic-paramagnetic transition above d_l have been studied analytically using functional RG and expansion in $\varepsilon = d_l - d$ to two-loop order^{38–40}. The effects of extended defects, free surfaces, and disorder correlation have been also investigated in Refs. 41–44.

The situation is even less understood in the case of an anisotropic distribution. The critical behavior of magnets with random anisotropy is usually described by the random anisotropy model (RAM) which was first introduced to describe magnetic properties of amorphous alloys of rare-earth compounds with aspherical electron distributions and transition metals⁶ (see also Refs. 45 and 46 for the experimental data). The Hamiltonian of RAM can be written as

$$\mathcal{H} = - \sum_{\langle \vec{R}, \vec{R}' \rangle} J \vec{S}_{\vec{R}} \vec{S}_{\vec{R}'} - D \sum_{\vec{R}} (\hat{x}_{\vec{R}} \vec{S}_{\vec{R}})^2, \quad (1)$$

where $J > 0$ is a short-range ferromagnetic interaction between $m > 1$ -component spins $\vec{S}_{\vec{R}} \equiv (S_{\vec{R}}^1, \dots, S_{\vec{R}}^m)$ located on sites of a d -dimensional hypercubic lattice, $\hat{x}_{\vec{R}}$ is a random unit vector indicating the direction of the local anisotropy axis on each site (see Fig. 1) and D is the anisotropy strength. Here we restrict ourselves to the case of uniaxial anisotropy corresponding to $D > 0$ and do not consider an easy-plane anisotropy emergent for $D < 0$.

Despite of extensive analytical and numerical studies even the nature of the low-temperature phase in three-dimensional random anisotropy systems is a controversial issue^{47,48}. While for completely isotropic distribution of a random local anisotropy axis the ferromagnetic ordering in the three-dimensional magnets is absent even in the limit of weak disorder controlled by the ratio D/J , it is not excluded for anisotropic distributions⁴⁸. There is an agreement between different approaches in the case of infinitely strong disorder, where appearance of a spin-glass order was observed^{49,50}. The situation is less clear for moderate and weak disorder. The question if the magnetic system can be ordered ferromagnetically, either it will be in a QLRO or a spin-glass phase is still controversial⁴⁸.

The standard way to study the critical behavior of model (1) analytically is to coarse grain it to a continuous effective models of ϕ^4 type which can be averaged over disorder using replicas and studied by field-theoretical RG methods^{51–53}. In the case of the isotropic distribution of the random anisotropy axis this leads to a model with three distinct ϕ^4 terms. As was shown in Refs. 54–56 this model has no stable physically accessible fixed point (FP) that is in agreement with the absence of the ferromagnetic state below $d = 4$ for isotropic distribution of anisotropies. In the case of random anisotropy with the cubic distribution, vectors $x_{\vec{R}}$ are aligned along

the edges of a m -dimensional hypercube and the effective Hamiltonian possesses four distinct ϕ^4 terms of different symmetries. In this case a continuous phase transition of random Ising universality class into a ferromagnetic state was predicted below $d = 4^{56–58}$. A more general model includes five distinct ϕ^4 terms⁵⁹. While this model was shown to have no stable FP to one-loop order it was recently argued that a stable FP appears at two-loop order in $d = 3^{60}$. Here we reconsider this problem by studying the model with a generic random anisotropy disorder to two-loop order using two different RG methods: minimal subtraction ($\overline{\text{MS}}$) scheme with the ε expansion and massive scheme directly in three dimension. We show that the both methods provide consistent pictures which exclude the possibility of a continuous phase transition in this model. This indicates the absence of a long-range order in the systems with a generic random anisotropy disorder.

The paper is organized as follows. Section II introduces the effective models for different distributions of random anisotropy axis. In Sec. III we renormalize the generic model with a trimodal distribution of anisotropies which includes five distinct ϕ^4 terms using the ε expansion and directly in three dimensions to two-loop order. In Sec. IV we analyze the corresponding RG flow using resummation techniques. We summarize our results in Sec. V.

II EFFECTIVE ϕ^4 HAMILTONIANS

We now map the spin lattice model (1) onto an effective ϕ^4 theory using the Hubbard-Stratonovich transformation and averaging over quenched disorder⁷ encoded by the local random vectors $\{\hat{x}_{\vec{R}}\}^{48,54}$. We use the replica trick⁶¹ introducing n copies of the original model and taking the limit of $n \rightarrow 0$ at the very end. One has to specify a particular distribution $p(\hat{x}_{\vec{R}})$ of the local random unit vectors $\hat{x}_{\vec{R}}$ in the m -dimensional target space. Let us consider three different cases.

In the case of the *isotropic distribution* any direction of the random unit vector $\hat{x}_{\vec{R}}$ is allowed with equal probability so that the probability distribution is given by

$$p_i(\hat{x}) = \frac{\Gamma(m/2)}{2\pi^{m/2}}, \quad (2)$$

where $\Gamma(x)$ is the Euler gamma-function. Averaging with this distribution leads to the effective Hamiltonian⁵⁴

$$\mathcal{H}_{\text{eff}} = - \int d^d r \left\{ \frac{1}{2} [\mu_0^2 |\phi|^2 + |\nabla \phi|^2] + \frac{u_0}{4!} |\phi|^4 + \frac{v_0}{4!} \sum_{\alpha=1}^n |\vec{\phi}^\alpha|^4 + \frac{z_0}{4!} \sum_{\alpha, \beta=1}^n \sum_{i, j=1}^m \phi_i^\alpha \phi_j^\alpha \phi_i^\beta \phi_j^\beta \right\}, \quad (3)$$

where $\phi = \{\vec{\phi}^\alpha(\vec{r})\}$ and $\vec{\phi}^\alpha(\vec{r}) = \{\phi_1^\alpha(\vec{r}), \dots, \phi_m^\alpha(\vec{r})\}$ is the n times replicated m -component order parameter, such that $|\phi|^2 = \sum_i^m \sum_\alpha^n |\phi_i^\alpha|^2$, and μ is the bare mass. The bare coupling constants $u_0 > 0$, $v_0 > 0$, $z_0 < 0$ satisfy $z_0/u_0 = -m$ (see also Table I).

In the case of the *cubic distribution* of the local anisotropy axis the random vector $\hat{x}_{\vec{R}}$ is allowed to point along one of the m axes of the hypercubic lattice with the probability distribution

$$p_c(\hat{x}) = \frac{1}{2m} \sum_{i=1}^m \left\{ \delta^{(m)}(\hat{x} - \hat{k}_i) + \delta^{(m)}(\hat{x} + \hat{k}_i) \right\}, \quad (4)$$

where $\hat{k}_i, \dots, \hat{k}_m$ are unit vectors along the axes and $\delta(y)$ is the Dirac delta-function. Averaging over the random variables $\{\hat{x}_{\vec{R}}\}$ for the *cubic distribution* one arrives at⁵⁴

$$\begin{aligned} \mathcal{H}_{\text{eff}} = & - \int d^d r \left\{ \frac{1}{2} [\mu_0^2 |\phi|^2 + |\nabla \phi|^2] + \frac{u_0}{4!} |\phi|^4 \right. \\ & + \frac{v_0}{4!} \sum_{\alpha=1}^n |\phi^{\vec{\alpha}}|^4 + \frac{w_0}{4!} \sum_{\alpha, \beta=1}^n \sum_{i=1}^m (\phi_i^\alpha)^2 (\phi_i^\beta)^2 \\ & \left. + \frac{y_0}{4!} \sum_{i=1}^m \sum_{\alpha=1}^n (\phi_i^\alpha)^4 \right\}. \end{aligned} \quad (5)$$

Here the bare coupling constants u_0, v_0, w_0 satisfy the conditions $u_0 > 0, v_0 > 0, w_0 < 0$ and $w_0/u_0 = -m$. Note that the term with coupling y_0 is not present in the bare microscopic model, but it is generated by the RG transformations so we have added it from the beginning. This, however, does not fix its sign.

Both the isotropic distribution and the cubic distribution can be combined into the so-called trimodal distribution^{62,63}

$$p(\hat{x}) = qp_i(\hat{x}) + (1-q)p_c(\hat{x}), \quad (6)$$

where the direction of \hat{x} is chosen either from the isotropic distribution with probability q or from the cubic distribution with the probability $(1-q)$. This leads to the effective Hamiltonian that contains all terms of the effective Hamiltonians (3) and (5)^{59,60}

$$\begin{aligned} \mathcal{H}_{\text{eff}} = & - \int d^d r \left\{ \frac{1}{2} [\mu_0^2 |\phi|^2 + |\nabla \phi|^2] + \frac{u_0}{4!} |\phi|^4 \right. \\ & + \frac{v_0}{4!} \sum_{\alpha=1}^n |\phi^{\vec{\alpha}}|^4 + \frac{w_0}{4!} \sum_{\alpha, \beta=1}^n \sum_{i=1}^m (\phi_i^\alpha)^2 (\phi_i^\beta)^2 \\ & \left. + \frac{y_0}{4!} \sum_{i=1}^m \sum_{\alpha=1}^n (\phi_i^\alpha)^4 + \frac{z_0}{4!} \sum_{\alpha, \beta=1}^n \sum_{i, j=1}^m \phi_i^\alpha \phi_j^\alpha \phi_i^\beta \phi_j^\beta \right\}, \end{aligned} \quad (7)$$

where the bare couplings satisfy $u_0 > 0, v_0 > 0, w_0 < 0, z_0 < 0$, while the sign of y_0 is arbitrary (see also Table I). However ratios z_0/u_0 and w_0/u_0 resulting from the trimodal distribution (6) are different from those for the distributions (2) and (5),

$$\frac{z_0}{u_0} = -\frac{2qm}{m(1-q)+2}, \quad (8)$$

$$\frac{w_0}{u_0} = -\frac{(1-q)(m+2)m}{m(1-q)+2}, \quad (9)$$

where for (8) with $q = 1$ we reproduce $z_0/u_0 = -m$ for the isotropic distribution, while for (9) with $q = 0$ we obtain $w_0/u_0 = -m$ for the cubic distribution.

TABLE I. The signs of the physical couplings for the effective Hamiltonians (3), (5), and (7). The two last lines correspond to the effective Hamiltonian obtained from the model (1) with the distribution (6) and the model (14) with the distribution (2), respectively.

Eqs.	u_0	v_0	w_0	y_0	z_0
(3)	> 0	> 0	0	0	< 0
(5)	> 0	> 0	< 0	∇	0
(1) with (6) \mapsto (7)	> 0	> 0	< 0	∇	< 0
(14) with (2) \mapsto (7)	> 0	> 0	∇	∇	< 0

It can be also shown that the effective Hamiltonian (7) can describe a more general local anisotropy axis distribution. Indeed, it can be derived for any distribution $p(\hat{x})$ provided that it has first two non-vanishing moments

$$M_{ij} = \int d^m \hat{x} p(\hat{x}) \hat{x}^i \hat{x}^j, \quad (10)$$

$$M_{ijkl} = \int d^m \hat{x} p(\hat{x}) \hat{x}^i \hat{x}^j \hat{x}^k \hat{x}^l, \quad (11)$$

which can be expressed as⁵⁸

$$M_{ij} = \frac{\delta_{ij}}{m} \quad (12)$$

$$M_{ijkl} = A(\delta_{ij}\delta_{kl} + \delta_{ik}\delta_{jl} + \delta_{il}\delta_{jk}) + B\delta_{ij}\delta_{ik}\delta_{il}. \quad (13)$$

Parameters A and B in (12) are determined by the precise form of the distribution $p(\hat{x})$ and satisfy the Cauchy inequalities $A(m+2) + B \geq 1/m$ and $3A + B \geq 1/m^2$. Note that the effective Hamiltonian (7) reduces to model (5) for $A = 0$.

The effective model (7) can be also derived by considering the system with the random single-ion cubic anisotropy given by

$$\begin{aligned} \mathcal{H} = & - \sum_{\vec{R}, \vec{R}'} J_{\vec{R}, \vec{R}'} \vec{S}_{\vec{R}} \vec{S}_{\vec{R}'} - D \sum_{\vec{R}} (\hat{x}_{\vec{R}} \vec{S}_{\vec{R}})^2 \\ & - V \sum_{\vec{R}} \sum_{i=1}^m (S_{\vec{R}}^i)^4, \end{aligned} \quad (14)$$

where V is the cubic anisotropy strength. It is straightforward to show that averaging (14) over the random variables $\{\hat{x}_{\vec{R}}\}$ with *isotropic distribution* leads to the effective Hamiltonian (7) with the bare couplings $u_0, v_0 > 0, z_0 < 0$ and $z_0/u_0 = -m$, while the sign of y_0 depends on the sign of V (see Table I). Similar to the case of the cubic distribution the coupling w_0 is not present in the bare model but it should be added, since it is generated by the RG transformations and may be of any sign.⁵⁹

Let us now discuss the conditions ensuring the physical stability of models (3), (5) and (7). The stability analysis can be carried out along the lines of Refs. 58 and 59. To that end we assume that the Hamiltonian

has a stable minimum characterized by the homogeneous order parameter M . We first consider the case when the symmetry of the ordered phase is broken with respect to (i) $\phi_i^\alpha = M$. Expanding the effective Hamiltonian (3) around this minimum we find that the region of stability reads⁵⁹

$$(i) \quad v_0 + nu_0 + nw_0 > 0. \quad (15)$$

In the case when symmetry is broken with respect to (ii) $\phi_i^\alpha = M\delta_{\alpha 1}\delta_{i1}$ one arrives at⁵⁹

$$(ii) \quad v_0 + u_0 + w_0 > 0. \quad (16)$$

If we consider that the symmetry is broken with respect to (iii) $\phi_i^\alpha = M\delta_{i1}$ and (iv) $\phi_i^\alpha = M\delta_{\alpha 1}$, we obtain the same conditions (15) and (16).

Repeating the same analysis for the effective Hamiltonian (5) we arrive at the following stability conditions⁵⁸

$$(i) \quad mnu_0 + mv_0 + nw_0 + y_0 > 0, \quad (17)$$

$$(ii) \quad u_0 + v_0 + w_0 + y_0 > 0, \quad (18)$$

$$(iii) \quad nu_0 + v_0 + nw_0 + y_0 > 0, \quad (19)$$

$$(iv) \quad mu_0 + mv_0 + w_0 + y_0 > 0. \quad (20)$$

Finally, we obtain the regions of stability of the effective Hamiltonian (7),

$$(i) \quad mnu_0 + mv_0 + nw_0 + y_0 + mnz_0 > 0, \quad (21)$$

$$(ii) \quad u_0 + v_0 + w_0 + y_0 + z_0 > 0, \quad (22)$$

$$(iii) \quad nu_0 + v_0 + nw_0 + y_0 + nz_0 > 0, \quad (23)$$

$$(iv) \quad mu_0 + mv_0 + w_0 + y_0 + mz_0 > 0. \quad (24)$$

As it was discussed in Ref. 59 in the replica limit $n \rightarrow 0$ the only relevant stability conditions appear to be those of replica symmetric configurations. Therefore in our case only conditions (i) and (iii) should be considered giving for $n = 0$

$$(i) \quad mv_0 + y_0 > 0 \quad (25)$$

$$(iii) \quad v_0 + y_0 > 0. \quad (26)$$

Before concluding this section let us mention that the Hamiltonian (7) is identical to

$$\begin{aligned} \mathcal{H}_{\text{eff}} = & - \int d^d r \left\{ \frac{1}{2} [\mu_0^2 |\phi|^2 + |\nabla \phi|^2] + \lambda_0 \sum_{i=1}^m \sum_{\alpha=1}^n (\phi_i^\alpha)^4 \right. \\ & + g_0 \sum_{i=1}^m \sum_{\alpha=1}^n (\phi_i^\alpha)^2 \sum_{k \neq i} (\phi_k^\alpha)^2 - \tilde{u}_0 \sum_{i=1}^m (\varphi_i^2)^2 \\ & \left. - 2\tilde{v}_0 \sum_{1 \leq i < k \leq m} \varphi_i^2 \varphi_k^2 - 2\tilde{w}_0 \sum_{1 \leq i < k \leq m} \left(\sum_{\alpha=1}^n \phi_i^\alpha \phi_k^\alpha \right)^2 \right\} \end{aligned} \quad (27)$$

with $\varphi_i^2 = \sum_{\alpha} (\phi_i^\alpha)^2$, which was introduced in Ref. 64 to study the influence of low-symmetry defects on the continuous phase transition. Comparing this expression with (7) one can see that recombining components ϕ_i^α in the Hamiltonian (7) transforms it to the Hamiltonian (27) with the following relations between the coupling constants $\lambda_0 = (v_0 + y_0)/4!$, $g_0 = v_0/4!$, $\tilde{u}_0 = -(u_0 + w_0 + z_0)/4!$, $\tilde{v}_0 = -u_0/4!$, and $\tilde{w}_0 = -z_0/4!$ (see Appendix A).

III FIELD-THEORY APPROACH

The field-theoretical RG approach completed by various techniques for resummation of asymptotic series^{51–53,65} is generally recognized as a powerful tool to get accurate estimates of critical exponents for systems with random bond/site disorder.^{1,66} It can be even applied to frustrated systems.^{67–70} Here we apply it to study the critical properties of the RAM with a generic distribution of random anisotropy axes.

The large scale behavior of the RAM with the effective Hamiltonian (7) can be described by one-particle irreducible ($1PI$) vertex functions which are defined as

$$\begin{aligned} & \delta \left(\sum_i^L p_i + \sum_j^N k_j \right) \hat{\Gamma}^{(L,N)}(\{p\}; \{k\}; \mu_0^2; \{\hat{\lambda}\}) \\ & = \int^{\Lambda_0} d^d R_1 \dots d^d R_L d^d r_1 \dots d^d r_N e^{i(\sum p_i R_i + \sum k_j r_j)} \\ & \times \langle \phi^2(R_1) \dots \phi^2(R_L) \phi(r_1) \dots \phi(r_N) \rangle_{1PI}^{\mathcal{H}_{\text{eff}}}, \end{aligned} \quad (28)$$

where $\{\hat{\lambda}\} = \{u_0, v_0, w_0, y_0, z_0\}$ are bare coupling constants, $\{p\}$, $\{k\}$ are external momenta, Λ_0 is a cut-off parameter, and μ_0 is a bare mass. In what follows we use the upper circle to denote the bare quantity.

In general the vertex functions (28) have a complicated tensor structure. As an example consider the vertex function $\hat{\Gamma}_{\alpha\beta\gamma\tau}^{(0,4)ijkl}$ which we will need to renormalize the theory. It is convenient to split it into the parts which possess the tensorial structure of the different terms in the bare model (7). This leads to

$$\begin{aligned} \hat{\Gamma}_{\alpha\beta\gamma\tau}^{(0,4)ijkl} = & \hat{\Gamma}_u^{(0,4)} S_{ijkl}^{\alpha\beta\gamma\tau} + \hat{\Gamma}_v^{(0,4)} S_{ijkl} F_{\alpha\beta\gamma\tau} \\ & + \hat{\Gamma}_w^{(0,4)} F_{ijkl} S_{\alpha\beta\gamma\tau} + \hat{\Gamma}_y^{(0,4)} F_{ijkl} F_{\alpha\beta\gamma\tau} \\ & + \hat{\Gamma}_z^{(0,4)} A_{ijkl}^{\alpha\beta\gamma\tau}, \end{aligned} \quad (29)$$

where we have introduced the tensors

$$\begin{aligned} F_{ijkl} & = \delta_{ij} \delta_{ik} \delta_{il}, \\ S_{ijkl} & = \frac{1}{3} (\delta_{ij} \delta_{kl} + \delta_{ik} \delta_{jl} + \delta_{il} \delta_{jk}), \\ S_{ijkl}^{\alpha\beta\gamma\tau} & = \frac{1}{3} (\delta_{ij} \delta_{kl} \delta_{\alpha\beta} \delta_{\gamma\tau} + \delta_{ik} \delta_{jl} \delta_{\alpha\gamma} \delta_{\beta\delta} + \delta_{il} \delta_{jk} \delta_{\alpha\tau} \delta_{\beta\gamma}), \\ A_{ijkl}^{\alpha\beta\gamma\tau} & = \frac{3}{2} S_{ijkl} S_{\alpha\beta\gamma\tau} - \frac{1}{2} S_{ijkl}^{\alpha\beta\gamma\tau}, \end{aligned}$$

and δ_{ab} is the Kronecker symbol.

A Renormalization

The functions (28) are divergent in the limit $\Lambda_0 \rightarrow \infty$ and have to be renormalized after a proper regularization. We apply two different renormalization schemes, the *massive scheme*⁷¹ and the $\overline{\text{MS}}$ *scheme*.⁷² To render the vertex functions finite we introduce the renormalization factors Z_ϕ for the field ϕ , Z_{ϕ^2} for the ϕ^2 -insertion,

and Z_{λ_i} for the coupling constants $\lambda_i = u, v, w, y, z$. The bare and renormalized vertex functions are related by

$$\Gamma^{(L,N)}(\{p\}; \{k\}; \{\lambda\}) = Z_\phi^{N/2} Z_{\phi^2}^L \mathring{\Gamma}^{(L,N)}(\{p\}; \{k\}; \{\mathring{\lambda}\}). \quad (30)$$

The renormalization schemes differ by the normalization conditions. In the massive scheme these conditions are formulated at zero external momenta and non-zero mass, and have the following form

$$\Gamma^{(0,2)}(k; -k; \mu^2; \{\lambda_i\}) \Big|_{k=0} = \mu^2, \quad (31a)$$

$$\frac{d}{dk^2} \Gamma^{(0,2)}(k; -k; \mu^2; \{\lambda_i\}) \Big|_{k=0} = 1, \quad (31b)$$

$$\Gamma_{\lambda_i}^{(0,4)}(\{k\}; \mu^2; \{\lambda_i\}) \Big|_{\{k\}=0} = \mu^{4-d} \lambda_i, \quad (31c)$$

$$\Gamma^{(1,2)}(p; k_1, k_2; \mu^2; \{\lambda_i\}) \Big|_{k_1=k_2=p=0} = 1. \quad (31d)$$

The renormalization factors Z_{λ_i} relate the bare couplings $\mathring{\lambda}_i$ to the renormalized ones:

$$\mathring{\lambda}_i = \mu^{4-d} \frac{Z_{\lambda_i}}{Z_\phi^2} \lambda_i. \quad (32)$$

The normalization conditions for the $\overline{\text{MS}}$ scheme are fixed at zero mass and given by

$$\Gamma^{(0,2)}(k, -k; \tilde{\mu}; \{\lambda_i\}) \Big|_{k=0} = 0, \quad (33a)$$

$$\frac{\partial}{\partial k^2} \Gamma^{(0,2)}(k, -k; \tilde{\mu}; \{\lambda_i\}) \Big|_{k^2=\tilde{\mu}^2} = 1, \quad (33b)$$

$$\Gamma_{\lambda_i}^{(0,4)}(\{k\}; \tilde{\mu}; \{\lambda_i\}) \Big|_{k_i k_j = \frac{\tilde{\mu}^2}{3} (4\delta_{ij} - 1)} = \tilde{\mu}^{4-d} \lambda_i, \quad (33c)$$

$$\Gamma^{(1,2)}(p; k, -k; \tilde{\mu}; \{\lambda_i\}) \Big|_{p^2=k^2=\tilde{\mu}^2, pk=-1/3\tilde{\mu}^2} = 1, \quad (33d)$$

where the renormalized couplings λ_i are

$$\mathring{\lambda}_i = \tilde{\mu}^{4-d} \frac{Z_{\lambda_i}}{Z_\phi^2} \lambda_i, \quad (34)$$

and $\tilde{\mu}$ is the external momentum scale parameter.

We now introduce the RG functions

$$\beta_{\lambda_i} = \frac{\partial \lambda_i}{\partial \ln \tilde{\mu}}, \quad \gamma_\phi = \frac{\partial Z_\phi}{\partial \ln \tilde{\mu}}, \quad \bar{\gamma}_{\phi^2} = -\frac{\partial \bar{Z}_{\phi^2}}{\partial \ln \tilde{\mu}},$$

where $\bar{Z}_{\phi^2} = Z_{\phi^2} Z_\phi$ and the derivatives are taken at fixed bare parameters. Here $\tilde{\mu}$ is the renormalized mass μ in the massive scheme and the scale parameter $\tilde{\mu}$ in the $\overline{\text{MS}}$ scheme. The β - and γ -functions characterize the change of the vertex functions under the RG transformation, and thus, allow one to calculate the scaling behavior in the critical region controlled by a FP

$$\beta_{\lambda_i}(\{\lambda_i^*\}) = 0, \quad i = 1, \dots, 5. \quad (35)$$

The FP solution $\{\lambda_i^*\}$ of Eqs. (35) describes the critical point of the system if it is stable and accessible from initial conditions. The FP is stable if all the eigenvalues $\{\omega_i\}$ of the stability matrix

$$B_{ij} = \frac{\partial \beta_{\lambda_i}}{\partial \lambda_j} \Big|_{\lambda_i=\lambda_i^*}, \quad (36)$$

have positive real parts ($\text{Re } \omega_i > 0$).

B RG functions

Applying the renormalization schemes (31) – (32), and (33) – (34) to the model (7) we obtain the RG functions to two-loop order. Introducing $\varepsilon = 4 - d$ the resulting β -function calculated within the both schemes can be written in the same form

$$\beta_{\lambda_i} = -\lambda_i(\varepsilon + \gamma_{\lambda_i} - 2\gamma_\phi), \quad (37)$$

once the one-loop integral $D_2 = \int \frac{d^d p}{(p^2+1)^2}$ appearing in the massive scheme is included in the redefinition of the coupling constants as $\lambda_i \rightarrow \lambda_i/D_2$, $\beta_{\lambda_i} \rightarrow \beta_{\lambda_i}/D_2$. The corresponding γ -functions are given by

$$\begin{aligned} u \gamma_u = & -\frac{1}{6} \left[(mn+8)u^2 + 2vw + 2vz + 2wz + 3z^2 + 2(m+2)uv + 2(n+2)uw + 6uy + 2(m+n+1)uz \right] \mathcal{E} \\ & - \frac{1}{9} \left[2(5mn+22)u^3 + 4v^2w + 4vw^2 + 4v^2z + 16vwz + 4w^2z + 2(m+8)vz^2 + 2(n+8)wz^2 + 3yz^2 \right. \\ & + 3(m+n+3)z^3 + 24(m+2)u^2v + 24(n+2)u^2w + 72u^2y + 24(m+n+1)u^2z + 6(m+2)uv^2 \\ & + 6(n+2)uw^2 + 36uwy + 18uy^2 + 12(n+4)uwz + 36uyz + 3(mn+m+n+15)uz^2 + 60uvw \\ & \left. + 36wvy + 12(m+4)wvz \right] \mathcal{I}, \end{aligned} \quad (38a)$$

$$\begin{aligned} v \gamma_v = & -\frac{1}{6} \left[(m+8)v^2 + 12uv + 4vw + 6vy + 2(m+5)vz + 6yz \right] \mathcal{E} - \frac{1}{9} \left[2(5m+22)v^3 + 6(mn+14)vu^2 \right. \\ & + 2(n+6)vw^2 + 36vwy + 18vy^2 + 24(m+5)uv^2 + 12(n+6)uvw + 108wvy + 68v^2w + 72v^2y \\ & + 12(3m+n+11)wvz + 4(7m+29)v^2z + 4(n+20)vwz + 72uyz + 132vyz + 24wyz + 18y^2z \\ & \left. + [(m+5)n + 17m + 67]vz^2 + 3(n+14)yz^2 \right] \mathcal{I}, \end{aligned} \quad (38b)$$

$$\begin{aligned}
w \gamma_w = & -\frac{1}{6} \left[(n+8)w^2 + 12uw + 4vw + 6wy + 2(n+5)wz + 6yz \right] \mathcal{E} - \frac{1}{9} \left[2(5n+22)w^3 + 6(mn+14)wu^2 \right. \\
& + 2(m+6)wv^2 + 36vwy + 18wy^2 + 24(n+5)uw^2 + 12(m+6)uvw + 108uwy + 68w^2v + 72w^2y \\
& + 12(m+3n+11)uwz + 4(7n+29)w^2z + 4(m+20)vwz + 72uyz + 132wyz + 24vyz + 18y^2z \\
& \left. + [(n+5)m + 17n + 67]wz^2 + 3(m+14)yz^2 \right] \mathcal{I}, \tag{38c}
\end{aligned}$$

$$\begin{aligned}
y \gamma_y = & -\frac{1}{6} \left[9y^2 + 8vw + 12vy + 12uy + 12wy + 6yz \right] \mathcal{E} - \frac{1}{9} \left[54y^3 + 96uvw + 4(m+18)v^2w + 252vwy \right. \\
& + 4(n+18)vw^2 + 6(mn+14)u^2y + 6(m+14)v^2y + 6(n+14)w^2y + 12(m+14)uwy + 144uy^2 \\
& + 12(n+14)uwy + 144vy^2 + 144wy^2 + 8(m+n+10)vwz + 12(m+n+7)uyz + 126y^2z \\
& \left. + 12(n+12)wyz + 12(m+12)vyz + 3(m+n+13)yz^2 \right] \mathcal{I}, \tag{38d}
\end{aligned}$$

$$\begin{aligned}
z \gamma_z = & -\frac{1}{6} \left[(m+n+4)z^2 + 12uz + 4vz + 4wz \right] \mathcal{E} - \frac{1}{9} \left[(2mn+5m+5n+27)z^3 + 6(mn+14)u^2z \right. \\
& + 2(m+6)v^2z + 2(n+6)w^2z + 12wyz + 2(5n+22)wz^2 + 24yz^2 + 44vwz + 12vyz \\
& \left. + 2(5m+22)vz^2 + 12(m+6)uvz + 12(n+6)uwz + 36uyz + 12(2m+2n+15)uz^2 \right] \mathcal{I}, \tag{38e}
\end{aligned}$$

$$\begin{aligned}
\gamma_\phi = & -\frac{1}{9} \left[(mn+2)u^2 + (m+2)v^2 + (n+2)w^2 + 3y^2 + \frac{mn+m+n+3}{2}z^2 + 2(m+2)uv \right. \\
& \left. + 2(n+2)uw + 6uy + 2(m+n+1)uz + 6vw + 6vy + 2(m+2)vz + 6wy + 2(n+2)wz + 6yz \right] \mathcal{J}, \tag{38f}
\end{aligned}$$

$$\begin{aligned}
\bar{\gamma}_{\phi^2} = & \frac{1}{6} \left[(mn+2)u + (m+2)v + (n+2)w + 3y + (m+n+1)z \right] \mathcal{E} \\
& - \frac{1}{3} \left[(mn+2)u^2 + (m+2)v^2 + (n+2)w^2 + 3y^2 + \frac{mn+m+n+3}{2}z^2 + 2(m+2)uv \right. \\
& \left. + 2(n+2)uw + 6uy + 2(m+n+1)uz + 6vw + 6vy + 2(m+2)vz + 6wy + 2(n+2)wz + 6yz \right] \mathcal{I}. \tag{38g}
\end{aligned}$$

The γ -functions (38) differ for the two renormalization schemes only by values of \mathcal{E} , \mathcal{I} , and \mathcal{J} . For the $\overline{\text{MS}}$ scheme one gets $\mathcal{E} = 1$, $\mathcal{I} = 1/4$, and $\mathcal{J} = -1/8$, while in the massive scheme $\mathcal{E} = \varepsilon$, $\mathcal{I} = \varepsilon(i_1 - 1/2)$, and $\mathcal{J} = \varepsilon i_2$. Here i_1 and i_2 are loop integrals which have to be computed in fixed dimension. In $d = 3$ they are given by $i_1 = 1/6$ and $i_2 = -2/27$,⁷³ while their values for general d can be found in Ref. 74.

While our main goal is to analyze the above RG functions in the replica limit of $n = 0$, corresponding to a disordered system with a generic random anisotropy distribution, it is also instructive to consider the model for arbitrary values of m and n . Before do that, let us check that the RG functions (37)-(38) satisfy the properties that follow from the original model (7) and reproduce properly the results known for reduced models.⁵⁸ These functions are expected to

- remain invariant under the simultaneous exchange $v \leftrightarrow w$ and $m \leftrightarrow n$;
- reproduce the RG functions of the mn model in the limit of $w = y = z = 0$ or $v = y = z = 0$ with $n \leftrightarrow m$ (see Refs.75–77 and references therein);

- reproduce the RG functions of the $(m \times n)$ -component cubic model in the limit of $v = w = z = 0$ (see Refs. 1, 75, 78, and 79 and references therein);

- reproduce the RG functions of the randomly dilute cubic model for $w = z = 0$ and $n = 0$,⁸⁰ and of the tetragonal model for $w = z = 0$ with $m = 2$;^{1,77}

- satisfy for $v = z = 0$, and $n = 0$ the identities

$$\begin{aligned}
\beta_u(u, 0, w, y, 0) + \beta_w(u, 0, w, y, 0) &= \beta_{RIM,u}(u+w, y), \\
\beta_y(u, 0, w, y, 0) &= \beta_{RIM,y}(u+w, y), \tag{39}
\end{aligned}$$

where $\beta_{RIM,u}(u, y)$ and $\beta_{RIM,y}(u, y)$ are the RG functions of the random Ising model (RIM);⁶⁶

- reproduce for $z = 0$ and $n = 0$ the RG functions of the RAM with cubic distribution obtained in Refs. 48, 56, and 58;

- reproduce for $w = y = 0$ and $n = 0$ the RG functions of the RAM with isotropic distribution obtained in Ref. 48 and 55;

- reproduce for $n = 0$ (after applying the transformation described in Appendix A) the $\overline{\text{MS}}$ β -functions for the crystal with low-symmetry defects derived in Ref. 64.

We have checked that our β -functions satisfy all these properties. Note, that the two-loop β -functions derived in Ref. 60 using a massive RG scheme do not satisfy all these conditions. For instance, the first property from the list above does not hold. As functions of Ref. 60 have been presented only for $n = 0$, to check this property we set $m = 0$ in β_v of Ref. 60 and substitute $v \leftrightarrow w$. Then we compare this with β_w of Ref. 60 where we also set $m = 0$. The obtained functions do not coincide, as they should. Moreover for $z = 0$ the RG-functions obtained in Ref. 60 do not match completely with (37)-(38) and with the functions derived in Ref. 57. They also do not reproduce the RG-functions calculated for the RAM with isotropic distribution of anisotropies in Ref. 55.

IV RG ANALYSIS

We can analyze the two-loop beta functions (37)-(38) either developing the ε -expansion, or directly in $d = 3$ by setting $\varepsilon = 1$ and considering the renormalized couplings as the expansion parameters.⁸¹ Since in the last case the

series in the coupling constants are asymptotic, in order to get reliable numerical data one has to apply appropriate resummation techniques.⁵¹⁻⁵³ In the next two subsections we will use both these approaches: we analyze our functions in the one-loop approximation using ε -expansion and then apply a resummation technique to the two-loop expressions in fixed space dimensions $d = 3$.

A One-loop approximation

Although our main interest is to analyze the RG-functions (37)-(38) in the limit of $n = 0$, the model under consideration has some applications also for non-zero n . The simplest example is the mn -vector model.^{75,76} At $m = 1$ and arbitrary n it reduces to the cubic model,^{1,75} while for $m = 2$, $n = 2$ and $n = 3$ it describes a class of special structural phase transitions.⁸² Another example is provided by the systems described by the reduced effective Hamiltonian (7) with $w = z = 0$. At $n = 0$ it corresponds to the randomly dilute cubic model⁸⁰ and for $m = 2$ and non-zero n it corresponds to the tetragonal model.¹

Let us first analyze the FPs of the RG functions (37)-(38) to the first-order in ε for arbitrary values of m and n . To this order the RG functions derived using the both schemes coincide and read

$$\beta_u = -\varepsilon u + \frac{1}{6} \left[(mn + 8)u^2 + 2vw + 2vz + 2wz + 3z^2 + 2(m + 2)uw + 2(n + 2)uw + 6uy + 2(m + n + 1)uz \right], \quad (40a)$$

$$\beta_v = -\varepsilon v + \frac{1}{6} \left[(m + 8)v^2 + 12uv + 4vw + 6vy + 2(m + 5)vz + 6yz \right], \quad (40b)$$

$$\beta_w = -\varepsilon w + \frac{1}{6} \left[(n + 8)w^2 + 12uw + 4vw + 6wy + 2(n + 5)wz + 6yz \right], \quad (40c)$$

$$\beta_y = -\varepsilon y + \frac{1}{6} \left[9y^2 + 8vw + 12vy + 12uy + 12wy + 6yz \right], \quad (40d)$$

$$\beta_z = -\varepsilon z + \frac{1}{6} \left[(m + n + 4)z^2 + 12uz + 4vz + 4wz \right]. \quad (40e)$$

The system of equations (40) has 32 solutions, from which the first 16 FPs has $z = 0$, and thus, describe a system with the cubic anisotropy distribution (4).

They are shown in lines I – XIII of Table II where we group the FPs with the same vanishing coupling constant. The first 14 FPs being taken in the limit of $n \rightarrow 0$ match those found in Ref. 54, 57, and 58. Note that the coordinates of several FPs have a pole at $n \rightarrow 0$ (e.g. FP XII and XIII in Table II), and thus, do not exist in this limit. The corresponding FPs with ($u^* \neq 0$, $y^* \neq 0$, $v^* = w^* = z^* = 0$ and $w^* \neq 0$, $y^* \neq 0$, $u^* = v^* = z^* = 0$) can be obtained in the next order of approximation with the help of $\sqrt{\varepsilon}$ -expansion.^{66,83} This also applies to the FP IX at $n = 0$ and $m = 2$.⁵⁷

The rest 16 FPs with $z^* \neq 0$ can be found along the lines of Ref. 64 (see Appendix B). Out of them, only six

can be expressed in the analytic form, the coordinates of the rest 10 FPs can be found only numerically. The FPs XIV – XVI with $z^* \neq 0$ which can be computed analytically are shown in Table II. Stability analysis of FPs listed in the Table II and other 10 FPs found numerically at $n = 0$ does not indicate that there are other stable FPs except for the FP III (for details see Appendix B). However, as it has been pointed out in Refs. 48, 55–58 where the reduced versions of the Hamiltonian (7) were analyzed using RG methods, this FP can not be reached along the RG flow starting from physical initial conditions. Indeed, the bare coupling constants satisfy conditions (8) and (9) and have fixed signs outlined below Eq. (7). The RG flow starting in this region will never reach FP III because of separatrices that restrict its basin of attraction.

TABLE II. FPs as a function of m and n to the first order in ε . Only 22 FPs (from all 32 FPs), which can be calculated analytically, are shown. The rest 10 FPs are discussed in Appendix B. Here, $x_{\pm} = (m+n-2 \pm \sqrt{(m+n-2)^2 - 12mn + 48})/(8-2mn)$; $A_{\pm}(m, n) = (m+n-2 + 2m\sigma(m, n) \pm \sqrt{(m+n-2 + 2m\sigma(m, n))^2 + 4(4-mn)(2\sigma(m, n) + 3)})/(8-2mn)$, $\sigma(m, n) = -(m-n+6)/(m+4)$; $A_{\pm}(n, m) = (m+n-2 + 2n\sigma(n, m) \pm \sqrt{(m+n-2 + 2n\sigma(n, m))^2 + 4(4-mn)(2\sigma(n, m) + 3)})/(8-2mn)$, $\sigma(n, m) = -(n-m+6)/(n+4)$; $\alpha_{\pm} = ((n-4)\gamma + 2m \pm \sqrt{((n-4)\gamma + 2m)^2 + 8(4-mn)\gamma})/(8-2mn)$, $\beta_{\pm} = -((4-n)\gamma + 8 \pm \sqrt{((4-n)\gamma + 8)^2 - 96\gamma})/6$, $\gamma = (m+4)/(n+4)$, $B_{\pm\pm} = 12\alpha_{\pm} + 6\beta_{\pm} + (n+8)\gamma + 4$, $\rho = m+n+4$, $\zeta(m, n) = (mn+8)(m+8)$, $\Sigma_{\pm}(m, n) = \sigma(m, n) + 3A_{\pm}(m, n)$.

FP	u^*	v^*	w^*	y^*	z^*
I.	0	0	0	0	0
II.	0	$\frac{6}{m+8}\varepsilon$	0	0	0
III.	$\frac{6}{mn+8}\varepsilon$	0	0	0	0
IV.	0	0	$\frac{6}{n+8}\varepsilon$	0	0
V.	0	0	0	$\frac{2}{3}\varepsilon$	0
VI.	$\frac{6(m-4)}{24(m+2)-\zeta(m,n)}\varepsilon$	$\frac{6(mn-4)}{\zeta(m,n)-24(m+2)}\varepsilon$	0	0	0
VII.	$\frac{6(n-4)}{24(n+2)-\zeta(n,m)}\varepsilon$	0	$\frac{6(mn-4)}{\zeta(n,m)-24(n+2)}\varepsilon$	0	0
VIII.	0	$\frac{2}{m}\varepsilon$	0	$\frac{2(m-4)}{3m}\varepsilon$	0
IX.	$\frac{2(m-4)}{(8-mn)m-16}\varepsilon$	$\frac{2(4-mn)}{(8-mn)m-16}\varepsilon$	0	$\frac{2}{3}\frac{(mn-4)(m-4)}{(mn-8)m+16}\varepsilon$	0
X.	$\frac{2(n-4)}{(8-mn)n-16}\varepsilon$	0	$\frac{2(4-mn)}{(8-mn)n-16}\varepsilon$	$\frac{2}{3}\frac{(mn-4)(n-4)}{(mn-8)n+16}\varepsilon$	0
XI. <i>a</i>	$\frac{6\alpha_+}{B_{++}}\varepsilon$	$\frac{6}{B_{++}}\varepsilon$	$\frac{6\gamma}{B_{++}}\varepsilon$	$\frac{6\beta_+}{B_{++}}\varepsilon$	0
<i>b</i>	$\frac{6\alpha_+}{B_{+-}}\varepsilon$	$\frac{6}{B_{+-}}\varepsilon$	$\frac{6\gamma}{B_{+-}}\varepsilon$	$\frac{6\beta_-}{B_{+-}}\varepsilon$	0
<i>c</i>	$\frac{6\alpha_-}{B_{-+}}\varepsilon$	$\frac{6}{B_{-+}}\varepsilon$	$\frac{6\gamma}{B_{-+}}\varepsilon$	$\frac{6\beta_+}{B_{-+}}\varepsilon$	0
<i>d</i>	$\frac{6\alpha_-}{B_{--}}\varepsilon$	$\frac{6}{B_{--}}\varepsilon$	$\frac{6\gamma}{B_{--}}\varepsilon$	$\frac{6\beta_-}{B_{--}}\varepsilon$	0
XII.	$\frac{2}{mn}\varepsilon$	0	0	$\frac{2}{3}\frac{mn-4}{mn}\varepsilon$	0
XIII.	0	0	$\frac{2}{n}\varepsilon$	$\frac{2}{3}\frac{n-4}{n}\varepsilon$	0
XIV. <i>a</i>	$\frac{6x_+}{\rho+12x_+}\varepsilon$	0	0	0	$\frac{6}{\rho+12x_+}\varepsilon$
<i>b</i>	$\frac{6x_-}{\rho+12x_-}\varepsilon$	0	0	0	$\frac{6}{\rho+12x_-}\varepsilon$
XV. <i>a</i>	$\frac{6A_+(m,n)\varepsilon}{\rho+4\Sigma_+(m,n)}$	$\frac{6\sigma(m,n)\varepsilon}{\rho+4\Sigma_+(m,n)}$	0	0	$\frac{6\varepsilon}{\rho+4\Sigma_+(m,n)}$
<i>b</i>	$\frac{6A_-(m,n)\varepsilon}{\rho+4\Sigma_-(m,n)}$	$\frac{6\sigma(m,n)\varepsilon}{\rho+4\Sigma_-(m,n)}$	0	0	$\frac{6\varepsilon}{\rho+4\Sigma_-(m,n)}$
XVI. <i>a</i>	$\frac{6A_+(n,m)\varepsilon}{\rho+4\Sigma_+(n,m)}$	0	$\frac{6\sigma(n,m)\varepsilon}{\rho+4\Sigma_+(n,m)}$	0	$\frac{6\varepsilon}{\rho+4\Sigma_+(n,m)}$
<i>b</i>	$\frac{6A_-(n,m)\varepsilon}{\rho+4\Sigma_-(n,m)}$	0	$\frac{6\sigma(n,m)\varepsilon}{\rho+4\Sigma_-(n,m)}$	0	$\frac{6\varepsilon}{\rho+4\Sigma_-(n,m)}$

We also computed the FPs for $m = 2$, $m = 3$ and $n = 1$, $n = 2$, $n = 3$ which are shown in Tables VII-XIV of Appendix B. We find that the FP III is also the only stable FP for $n = 1$, while for $n > 1$ there is no stable FP.

Therefore, the exhaustive analysis of the one-loop β functions indicates the absence of a continuous phase transition of the random anisotropy with a generic random axis distribution. In the next subsection we show that this conclusion holds also at the two-loop order contrary to the claim of Ref. 60.

B Two-loop approximation

As it was shown for the model with three coupling constants the straightforward calculation of the FP coordinates using the asymptotic series is not very accurate.⁵⁵ To extract the reliable information, we apply the Padé-Borel resummation method⁸⁴ which is described in the Appendix C.

In this subsection we analyze the β -functions (37)-(38) in the replica limit of $n = 0$ for $m = 2$, $m = 3$. To that end we resume them using the Padé-Borel method (C.3) and then solve the obtained system of five non-linear equations. The computed FPs are shown in Tables III, IV (for the massive RG scheme) and in Tables V, VI (for the $\overline{\text{MS}}$ scheme). There we list only the FPs with real coordinates. In the limiting cases, the obtained results reproduce the known ones.^{48,55-57}

Unlike the one-loop approximation, where we know the number of solutions, here we solve the system of non-algebraic equations and thus the number of FPs is unknown in advance. This procedure may lead to spurious FPs which are not perturbative in ε , i.e. do not coincide with the Gaussian FP in $d = 4$ and which appear and disappear once one increases the number of loops taken into account. If such a solution exists and turns out to be stable, one needs a careful analysis to check if this is a real or spurious FP, see e.g. Refs. 67-69. Fortunately, we do not find such solutions, since all FPs turn out to

be unstable. For the sake of convenience we adopt the classification of one-loop FPs introduced in Table II by regrouping all the two-loop FPs of the same symmetry found using the resummation technique.

Note that in this approximation the FP coordinates are renormalization scheme dependent and differ for the massive and $\overline{\text{MS}}$ schemes.⁵²

We consider only the physical FPs with couplings $u^* > 0$, $v^* > 0$, $z^* < 0$, and any w^* and y^* (see Table II). Among all FPs there is only one stable physical FP. This is the “polymer” $\mathcal{O}(n=0)$ FP, which is stable for any m (point III in Tables III – VI), but unfortunately this FP is unreachable from physical initial conditions. The FP with coordinates $u^* = v^* = z^* = 0$, $w^* < 0$, and $y^* > 0$, which corresponds to the stable FP of the Hamiltonian (5), has one negative stability eigenvalue associated with coupling z . Thus the stable and physically accessible FP of the RAM with the cubic distribution of local anisotropy axis (4) (FP XIII of Tables III – VI) becomes unstable with respect to this perturbation.

Let us compute the corresponding crossover exponent ϕ_z which is related to the stability eigenvalue

$$\omega_z = \left. \frac{\partial \beta_z}{\partial z} \right|_{0,0,w^*,y^*,0}. \quad (41)$$

as $\phi_z = -\omega_z \nu$, where ν is the correlation length critical exponent calculated in this fixed point (see e.g. 48 and 57). In the massive scheme we find

$$\omega_z = -1.1947, \quad \phi_z \equiv -\omega_z \nu = 0.8071, \quad (42)$$

while in the $\overline{\text{MS}}$ scheme we obtain

$$\omega_z = -1.0747, \quad \phi_z \equiv -\omega_z \nu = 0.7173. \quad (43)$$

The difference between the results computed using different renormalization schemes provides an estimation of the error bars for the critical exponent values.

It is instructive to compare our result with the six-loop estimate obtained within the massive RG scheme in Ref. 58, where the RG dimension $y_z = -\omega_z$ calculated from a certain scaling operator of the cubic model is $y_z = 1.16(6)$, and the crossover exponent is $\phi_z = 0.79(4)$. Surprisingly our two-loop estimates of these universal quantities are very close to those obtained within the six-loop approximation. Such high values of crossover exponents mean that the presence of even a very small z - contribution in (7) leads to high instability of the FP XIII.

The analysis of the two-loop β functions calculated using two different renormalization schemes gives a solid evidence of the fact that there are no FPs that are simultaneously stable and reachable from physical initial conditions for the Hamiltonian (7).

V CONCLUSIONS

We have studied the effect of generic structural disorder on the critical properties of magnets. To that end

we have applied a field-theoretical RG to the RAM with a trimodal distribution of random anisotropy axes which combines the isotropic and cubic distributions. We have derived the RG functions for the model (7) with arbitrary m and n to two-loop order. We have used two different regularization schemes, the $\overline{\text{MS}}$ scheme and the massive scheme, in order to check the validity of our results. We have verified that the RG functions reproduce the results known for the limiting cases of the isotropic and cubic distributions. Applying the Padé-Borel resummation technique we have identified all FPs of the RG flow and studied their stability. This reveals no stable FP in both schemes except for the FP III, which is inaccessible from physical initial conditions. This indicates the absence of a continuous phase transition at variance with the claim of Ref. 60 about the existence of a continuous phase transition of a new universality class. However, as we shown the conclusion of Ref. 60 was based on erroneous two-loop β - functions which neither possess the required symmetry properties nor match with the known results.

Our results show that the magnetic materials with general distribution of random anisotropy axes do not undergo a continuous phase transition. Although the RG analysis of the type presented here is not able to make a solid conclusion about the origin of the low-temperature phase, our result in combination with other theoretical and numerical data (see in particular the review of results in the introductory part of this paper) gives one more argument in favor of an absence of a low-temperature long-range ordered state.⁴⁸ This is in contrast to the anisotropic distribution of random anisotropy axes where the ferromagnetic order persists in the presence of structural disorder.⁸⁵ This does not exclude existence of a QLRO phase similar to that in the case of isotropic distribution of random anisotropies,³⁷ which, however, is not accessible within our method.

Beside the RAM with a generic random anisotropy distribution, the RG functions (38), which we have obtained for general m and n , can be also used to study the critical properties of other models such as the dilute cubic model⁸⁰ and the tetragonal model.¹

ACKNOWLEDGMENT

Yu. H. and M. D. thank Reinhard Folk and Juan J. Ruiz-Lorenzo for numerous discussions and collaboration. M.D. acknowledges support from Polish National Agency for Academic Exchange through the grant PPN/ULM/2019/00160

Appendix A

Here we present the relations between our two-loop β -functions computed within $\overline{\text{MS}}$ scheme in the limit of $n = 0$ ($\beta_u, \beta_v, \beta_w, \beta_y, \beta_z$) and the β -functions computed in Ref. 64 for the phase transition in the crystals with low-symmetry point defects at replica limit ($\beta_\lambda, \beta_g, \beta_{\bar{u}}, \beta_{\bar{v}}, \beta_{\bar{w}}$). They read

TABLE III. FPs for $m = 2$ computed in the massive scheme to two-loop order.

FP	u^*	v^*	w^*	y^*	z^*
I	0	0	0	0	0
II	0	0.9107	0	0	0
III	1.1857	0	0	0	0
IV	0	0	1.1857	0	0
V	0	0	0	1.0339	0
VI	-0.0322	0.9454	0	0	0
VII	2.1112	0	-2.1112	0	0
VIII	0	1.5509	0	-1.0339	0
IX	-0.4401	2.3900	0	-1.5933	0
X. α	-0.1387	0	-0.2667	1.5509	0
β	0.6678	0	-0.6678	1.0339	0
XI. α	-0.0899	-0.0081	-0.3262	1.5727	0
β	0.3486	-0.2398	-0.4969	1.4538	0
γ	0.4128	0.5013	0.7676	-0.5706	0
δ	0.4755	1.2862	1.1146	-2.4093	0
ϵ	1.9951	-1.7745	-2.4995	1.9710	0
XII	0.4755	0	0	-2.4093	0
XIII	0	0	-0.4401	1.5933	0
XIV. α	0.5349	0	0	0	0.5325
β	1.4650	0	0	0	-1.6278
XV. α	0.3427	2.0830	0	0	-1.1498
β	0.7991	0.7341	0	0	-0.5360
XVI. α	0.5929	0	-1.1857	0	1.1857
β	1.0556	0	2.1112	0	-2.1112
XVII. α	-0.2201	2.3900	0.4401	-1.5933	-0.4401
β	0.1106	1.9238	0.5040	-1.4409	-0.5040
γ	0.3339	1.5509	0.6678	-1.0339	-0.6678
δ	0.7139	1.1670	2.4589	-1.9465	-2.4077
ϵ	0.7394	1.1381	2.4016	-1.8889	-2.4016
ζ	0.7971	-0.3573	-0.7735	0.5750	0.7735

TABLE IV. FPs for $m = 3$ computed in the massive scheme to two-loop order.

FP	u^*	v^*	w^*	y^*	z^*
I	0	0	0	0	0
II	0	0.8102	0	0	0
III	1.1857	0	0	0	0
IV	0	0	1.1857	0	0
V	0	0	0	1.0339	0
VI	0.1733	0.6460	0	0	0
VII	2.1112	0	-2.1112	0	0
VIII	0	0.8394	0	-0.0485	0
IX	0.1695	0.7096	0	-0.1022	0
X. α	0.6678	0	-0.6678	1.0339	0
β	-0.1387	0	-0.2667	1.5509	0
XI. α	-0.0879	-0.0070	-0.3295	1.5731	0
β	0.2833	-0.1901	-0.5381	1.5365	0
γ	0.4371	0.4027	0.7289	-0.5051	0
δ	0.5704	1.0219	1.1630	-2.2717	0
XII	0.4755	0	0	-2.4093	0
XIII	0	0	-0.4401	1.5933	0
XIV	0.5386	0	0	0	0.4431
XV	0.8450	0.5934	0	0	-0.4506
XVI	0.5753	0	-0.4570	0	0.6462
XVII	0.8962	-0.3497	-0.8276	0.7597	0.5187

TABLE V. FPs for $m = 2$ computed in the $\overline{\text{MS}}$ scheme to two-loop order.

FP	u^*	v^*	w^*	y^*	z^*
I	0	0	0	0	0
II	0	1.1415	0	0	0
III	1.5281	0	0	0	0
IV	0	0	1.5281	0	0
V	0	0	0	1.3146	0
VI	0.1429	0.9923	0	0	0
VII	2.5382	0	-2.5382	0	0
VIII. α	0	-0.6347	0	2.1354	0
β	0	1.9719	0	-1.1346	0
IX. α	-0.2506	2.4494	0	-1.6330	0
β	-0.2273	0.0544	0	1.5335	0
X. α	-0.0328	0	-0.2134	1.6275	0
β	0.7311	0	-0.7311	1.3146	0
XI. α	-0.1940	0.0306	-0.0400	1.5737	0
β	-0.0228	-0.0003	-0.2247	1.6294	0
γ	0.2670	-0.1330	-0.4058	1.6247	0
δ	0.5580	0.6121	0.9464	-0.6988	0
ϵ	0.5580	1.5704	1.2423	-2.7081	0
ζ	2.3469	-2.1042	-2.8990	2.3216	0
XII	-0.2506	0	0	1.6330	0
XIII	0	0	-0.2506	1.6330	0
XIV. α	0.7060	0	0	0	0.6578
β	1.6637	0	0	0	-1.8212
XV. α	0.4515	2.2913	0	0	-1.2002
β	1.0126	0.9058	0	0	-0.6522
XVI. α	0.7641	0	-1.5281	0	1.5281
β	1.2691	0	2.5382	0	-2.5382
XVII. α	-0.1253	2.4494	0.2506	-1.6330	-0.2506
β	0.1053	2.2733	0.4659	-1.6032	-0.4659
γ	0.3656	1.9719	0.7311	-1.3146	-0.7311
δ	0.6551	1.5440	3.1917	-2.6796	-2.7467
ϵ	0.8821	1.2846	2.6931	-2.1470	-2.6931
ζ	1.0333	-0.4429	-0.9614	0.7097	0.9614

$$\beta_\lambda(\lambda, g, \tilde{u}, \tilde{v}, \tilde{w}) = -\frac{1}{96} \left[\beta_y(-48\tilde{v}, 48g, 48(\tilde{v}+\tilde{w}-\tilde{u}), 48(\lambda-g), -48\tilde{w}) + \beta_v(-48\tilde{v}, 48g, 48(\tilde{v}+\tilde{w}-\tilde{u}), 48(\lambda-g), -48\tilde{w}) \right], \quad (\text{A.1})$$

$$\beta_g(\lambda, g, \tilde{u}, \tilde{v}, \tilde{w}) = -\frac{1}{96} \beta_v(-48\tilde{v}, 48g, 48(\tilde{v}+\tilde{w}-\tilde{u}), 48(\lambda-g), -48\tilde{w}), \quad (\text{A.2})$$

$$\beta_{\tilde{u}}(\lambda, g, \tilde{u}, \tilde{v}, \tilde{w}) = \frac{1}{96} \left[\beta_u(-48\tilde{v}, 48g, 48(\tilde{v}+\tilde{w}-\tilde{u}), 48(\lambda-g), -48\tilde{w}) + \beta_w(-48\tilde{v}, 48g, 48(\tilde{v}+\tilde{w}-\tilde{u}), 48(\lambda-g), -48\tilde{w}) + \beta_z(-48\tilde{v}, 48g, 48(\tilde{v}+\tilde{w}-\tilde{u}), 48(\lambda-g), -48\tilde{w}) \right], \quad (\text{A.3})$$

$$\beta_{\tilde{v}}(\lambda, g, \tilde{u}, \tilde{v}, \tilde{w}) = \frac{1}{96} \beta_u(-48\tilde{v}, 48g, 48(\tilde{v}+\tilde{w}-\tilde{u}), 48(\lambda-g), -48\tilde{w}), \quad (\text{A.4})$$

$$\beta_{\tilde{w}}(\lambda, g, \tilde{u}, \tilde{v}, \tilde{w}) = \frac{1}{96} \beta_z(-48\tilde{v}, 48g, 48(\tilde{v}+\tilde{w}-\tilde{u}), 48(\lambda-g), -48\tilde{w}). \quad (\text{A.5})$$

Appendix B

In this Appendix we give details on finding the FPs with $z^* \neq 0$ to one-loop order. There are 16 such FPs which can be found along the lines of Ref. 64. Introducing

variables

$$a = u/z, \quad b = v/z, \quad c = w/z, \quad d = y/z, \quad (\text{B.1})$$

we arrive at the system of nonlinear algebraic equations

TABLE VI. FPs for $m = 3$ computed in the $\overline{\text{MS}}$ scheme to two-loop order.

FP	u^*	v^*	w^*	y^*	z^*	
I	0	0	0	0	0	
II	0	1.0016	0	0	0	
III	1.5281	0	0	0	0	
IV	0	0	1.5281	0	0	
V	0	0	0	1.3146	0	
VI	0.3411	0.6965	0	0	0	
VII	2.5382	0	-2.5382	0	0	
VIII	0	0.8568	0	0.2270	0	
IX. α	-0.2126	0.0341	0	1.5407	0	
	β	0.3405	0.7275	0	-0.0511	0
X. α	0.7311	0	-0.7311	1.3146	0	
	β	-0.0328	0	-0.2134	1.6275	0
XI. α	-0.0225	-0.0003	-0.2250	1.6294	0	
	β	-0.1787	0.0175	-0.0503	1.5838	0
	γ	0.1822	-0.0744	-0.3824	1.6437	0
	δ	0.5908	0.4827	0.8871	-0.6083	0
	ϵ	0.6928	1.2393	1.3072	-2.5420	0
XII	-0.2506	0	0	1.6330	0	
XIII	0	0	-0.2506	1.6330	0	
XIV	0.7126	0	0	0	0.5377	
XV	1.0728	0.7310	0	0	-0.5483	
XVI	0.7555	0	-0.5382	0	0.7820	
XVII	1.1512	-0.4311	-1.0150	0.9279	0.6426	

$$(m+4)b^2 + (6d+m-n+6)b + 6d = 0, \quad (\text{B.2a})$$

$$(n+4)c^2 + (6d+n-m+6)c + 6d = 0, \quad (\text{B.2b})$$

$$9d^2 + (8b+8c-m-n+2)d + 8bc = 0, \quad (\text{B.2c})$$

$$(4-mn)a^2 - (2mb+2nc+6d+m+n-2) - (2bc+2b+2c+3) = 0, \quad (\text{B.2d})$$

$$\varepsilon - z(2a+2b/3+2c/3+(m+n+4)/6) = 0. \quad (\text{B.2e})$$

Solving the system of the first three equations (B.2a) – (B.2c) with respect to b , c , and d , we obtain for the case $n \neq 0$ eight sets of roots. Substituting each set (b, c, d) into the quadratic equation (B.2d) we find two values of a leading to 16 sets (a, b, c, d) . The corresponding value of z for each set is found from the linear equation (B.2e). Subsequently, variables u, v, w, y can be found using (B.1). Out of all 16 solutions, only six can be expressed in the analytic form. These are related to three solutions of the system of equations (B.2a) – (B.2c):

$$\begin{aligned} b = c = d = 0, \\ b = -\frac{m-n+6}{m+4}, \quad c = d = 0, \\ b = 0, \quad c = -\frac{n-m+6}{n+4}, \quad d = 0. \end{aligned} \quad (\text{B.3})$$

These FPs are denoted by XIV – XVI in Table II. Their coordinates in the limit $n \rightarrow 0$ reproduce the results obtained in Refs. 55 and 64. The coordinates of the rest 10

FPs can be found only numerically. Let us note that the coordinates of these FPs for the considered values of m and n attain complex values in general. Finally, we have to solve the fifth-order equation for b . The solution of the system of equations (B.2a) – (B.2c) for non-vanishing n , reduces to the solution of the following fifth-order equation for b :

$$\begin{aligned} & (m+4)(3m-4)(3mn-4m-4n+16)b^5 \\ & + [m^3(39n-68) + m^2(-15n^2+198n+456) \\ & + 8m(n^2-56n-72) + 16(n^2+6n+24)]b^4 \\ & + [m^3(67n-148) + m^2(-34n^2+576n+1536) \\ & + m(7n^3-96n^2-996n-2960) - 4n^3+96n^2 \\ & + 560n+1728]b^3 + [3m^3(19n-52) + m^2(-19n^2 \\ & + 662n+2056) - m(5n^3+88n^2+1060n+4112) \\ & - n^4+30n^3+60n^2+744n+2016]b^2 + 4[m^3(6n \\ & - 20) + m^2(n^2+82n+312) - 4m(n^3-5n^2 \\ & + 28n+164) + n^4-10n^3+20n^2+8n+352]b \\ & + 4(m+n-2)(m^2(n-4)+4m(5n+16)-n^3 \\ & - 4n^2-28n-48) = 0. \end{aligned} \quad (\text{B.4})$$

Then c and d can be found from:

$$\begin{aligned} c = & (b((3m-4)b+5m-n-2) + 2(m+n-2)) \\ & \times \frac{((m+4)b+m-n+6)}{6(b+1)(b(m-2)+m-n)}, \end{aligned} \quad (\text{B.5})$$

$$d = -b \frac{(m+4)b+m-n+6}{6(b+1)}. \quad (\text{B.6})$$

Other parameters can be found using the procedure described above.

The task is simplified in the case $n = 0$, since we can extract separate set of roots $b = -2$, $c = -(m+2)/4$, $d = (m+2)/3$ in addition to (B.3). Therefore we can find the rest 4 roots solving the fourth-order equation

$$\begin{aligned} & (3m-4)(m^2-16)b^4 + (m-4)(m(11m+2)-8)b^3 \\ & + [m(3m(5m-36)+196)-112]b^2 \\ & + (m-2)(m(9m-88)+76)b \\ & + 2(m-2)((m-16)m+12) = 0. \end{aligned} \quad (\text{B.7})$$

that can be done analytically.⁸⁶

The rest FPs which can be computed only numerically are shown in Tables VII – XIV for several values of m and n . Analysis of these FPs indicates the absence of stable FPs for $m = 2$, $m = 3$ in the cases $n = 2$ and $n = 3$ (Tables XI–XIV). For other values of n ($n = 0$ and $n = 1$) for $m = 2$ and $m = 3$ only FP III is stable.

Appendix C

Here, we present the resummation procedure used in our study. The RG functions calculated within

TABLE VII. FPs to the first order in ε for $m = 2$ and $n = 0$.

FP	u^*	v^*	w^*	y^*	z^*
I	0	0	0	0	0
II	0	0.6	0	0	0
III	0.75	0	0	0	0
IV	0	0	0.75	0	0
V	0	0	0	0.6667	0
VI	-0.75	1.5	0	0	0
VII	1.5	0	-1.5	0	0
VIII	0	1.	0	-0.6667	0
X	0.5	0	-0.5	0.6667	0
XI	1.5	2.3028	3.4542	-8.1407	0
	0.2295	0.3524	0.5285	-0.3987	0
	0.3631	-0.3153	-0.4730	1.1148	0
	1.5	-1.3028	-1.9542	1.4741	0
XIV	0.3170	0	0	0	0.3660
	1.1830	0	0	0	-1.3660
XV	0.2592	-5.7784	0	0	4.3338
	0.5208	0.4984	0	0	-0.3738
XVI	0.375	0	-0.75	0	0.75
	0.75	0	1.5	0	-1.5
XVII	0.25	1.	0.5	-0.6667	-0.5
	0.1266	1.3568	0.4730	-1.1148	-0.4730
	3.2262	-9.9050	-3.4530	8.1381	3.4530
	0.5229	0.9083	1.9541	-1.4740	-1.9541
	0.4938	-0.2457	-0.5285	0.3987	0.5285

TABLE VIII. FPs to the first order in ε for $m = 3$ and $n = 0$.

FP	u^*	v^*	w^*	y^*	z^*
I	0	0	0	0	0
II	0	0.5455	0	0	0
III	0.75	0	0	0	0
IV	0	0	0.75	0	0
V	0	0	0	0.6667	0
VI	-0.1875	0.75	0	0	0
VII	1.5	0	-1.5	0	0
VIII	0	0.6667	0	-0.2222	0
IX	-0.25	1.	0	-0.3333	0
X	0.5	0	-0.5	0.6667	0
XI	0.9313	1.1375	1.9906	-4.2749	0
	0.2411	0.2945	0.5153	-0.3657	0
	0.3691	-0.3453	-0.6043	1.2979	0
	2.8187	-2.6375	-4.6156	3.2749	0
XIV	0.3158	0	0	0	0.3158
	2.25	0	0	0	-3.
XV	0.1423	-2.9716	0	0	2.3113
	0.5488	0.4055	0	0	-0.3154
XVI	0.3462	0	-0.3462	0	0.4615
	1.5	0	2.25	0	-3.
XVII	0.3	0.8	0.5	-0.667	-0.4
	0.2934	0.8369	0.4968	-0.7111	-0.4079
	0.1644	1.2038	2.8826	-2.6746	-1.7597
	0.5678	-0.2432	-0.5823	0.5403	0.3555
	760.35	-3077.7	-1826.85	2615.25	1500.

TABLE IX. FPs to the first order in ε for $m = 2$ and $n = 1$.

FP	u^*	v^*	w^*	y^*	z^*
I	0	0	0	0	0
II	0	0.6	0	0	0
III	0.6	0	0	0	0
IV	0	0	0.6667	0	0
V	0	0	0	0.6667	0
VI	3.	-3.	0	0	0
VII	1	0	-0.6667	0	0
VIII	0	1.	0	-0.6667	0
IX	1.	-1.	0	0.6667	0
X	0.6	0	-0.4	0.4	0
XI	0.5455	0.4545	0.5455	-1.2121	0
	0.3273	0.2727	0.3273	-0.3273	0
	0.4545	-0.4545	-0.5455	1.2121	0
	1.3636	-1.3636	-1.6364	1.6364	0
XII	1.	0	0	-0.6667	0
XIII	0	0	2.	-2.	0
XIV	0.36	0	0	0	0.24
	1.2	0	0	0	-1.2
XV	0.2308	-1.6154	0	0	1.3846
	0.5538	0.3231	0	0	-0.2769
XVI	0.3333	0	-0.6667	0	0.6667
	0.6667	0	0.6667	0	-0.6667
XVII	0.1818	1.3637	0.5455	-1.2122	-0.5455
	0.8182	-1.3636	-0.5455	1.2121	0.5455
	0.5454	1.0910	1.6365	-1.6365	-1.6365
	0.4909	-0.2182	-0.3273	0.3273	0.3273
	0.4	0.6	0.4	-0.4	-0.4
	1.	-3.	-2.	2.	2.

a field-theoretical approach are represented by asymptotic series. They are characterized by a factorial growth of the coefficients implying a zero radius of convergence.^{51,52} Extracting from them a physical information requires application of resummation methods, such as the Borel resummation accompanied by certain additional procedures.⁸⁷ We use Padé-Borel resummation technique⁸⁴ for “resolvent” series, where an auxiliary variable is introduced and Borel image of this series is extrapolated by a rational Padé approximant $[K/L]$ ⁸⁸ for this new variable. First, for a given initial polynomial

$$\beta(u, v, w, y, z) = \sum_{1 \leq i+j+k+l+p \leq 5} a_{i,j,k,l,p} u^i v^j w^k y^l z^p, \quad (\text{C.1})$$

we build “resolvent” polynomial introducing an auxiliary variable λ in the following way:

$$F(u, v, w, y, z; \lambda) = \sum_{1 \leq i+j+k+l+p \leq 5} a_{i,j,k,l,p} u^i v^j w^k y^l z^p \lambda^{i+j+k+l+p-1}, \quad (\text{C.2})$$

TABLE X. FPs to the first order in ε for $m = 3$ and $n = 1$.

FP	u^*	v^*	w^*	y^*	z^*
I	0	0	0	0	0
II	0	0.5455	0	0	0
III	0.5455	0	0	0	0
IV	0	0	0.6667	0	0
V	0	0	0	0.6667	0
VI	6.	-6.	0	0	0
VII	0.6667	0	-0.2222	0	0
VIII	0	0.6667	0	-0.2222	0
IX	2.	-2.	0	0.6667	0
X	0.5455	0	-0.1818	0.1818	0
XI	0.4912	0.1754	0.2456	-0.4678	0
	0.4019	0.1435	0.2010	-0.2010	0
	0.5263	-0.5263	-0.7368	1.4035	0
	1.5790	-1.5790	-2.2105	2.2105	0
XII	0.6667	0	0	-0.2222	0
XIII	0	0	2.	-2.	0
XIV	0.4091	0	0	0	0.1364
	1.5	0	0	0	-1.5
XV	0.1667	-1.3333	0	0	1.1667
	0.5303	0.1212	0	0	-0.1061
XVI	0.3889	0	-0.2222	0	0.2778
	0.8333	0	0.6667	0	-0.8333
XVII	0.4091	0.2727	0.2727	-0.2727	-0.1364
	1.5	-3.	-3.	3.	1.5
	0.3889	0.5556	0.3333	-0.5556	-0.2778
	0.8333	-1.6667	-1.	1.6667	0.8333
	0.1667	0.9998	2.3332	-2.3332	-1.1666
	0.5303	-0.0909	-0.2121	0.2121	0.1061

TABLE XI. FPs to the first order in ε for $m = 2$ and $n = 2$.

FP	u^*	v^*	w^*	y^*	z^*
I	0	0	0	0	0
II	0	0.6	0	0	0
III	0.5	0	0	0	0
IV	0	0	0.6	0	0
V	0	0	0	0.6667	0
VIII	0	1.	0	-0.6667	0
XIII	0	0	1.	-0.6667	0
XVII	0.9	-1.2	-1.2	1.2	0.6
	0.3	0.6	1.2	-1.2	-0.6
	0.3	1.2	0.6	-1.2	-0.6
	0.5	1.	1.	-1.3333	-1.
	0.5	-1.	1.	0.6667	1.

It satisfies the relation $F(u, v, w, y, z; \lambda=1) = \beta(u, v, w, y)$. The Borel image for this series reads

$$F^B(u, v, w, y, z; \lambda) = \sum_{1 \leq i+j+k+l+p \leq 5} \frac{a_{i,j,k,l,p} u^i v^j w^k y^l z^p}{(i+j+k+l+p-1)!} \times \lambda^{i+j+k+l+p-1}. \quad (\text{C.3})$$

Subsequently series (C.3) is approximated by the Padé-approximant $[K/L](\lambda)$, since we are in two-loop approximation we can use only two approximants $[1/1](\lambda)$,

TABLE XII. FPs to the first order in ε for $m = 3$ and $n = 2$.

FP	u^*	v^*	w^*	y^*	z^*
I	0	0	0	0	0
II	0	0.5455	0	0	0
III	0.4286	0	0	0	0
IV	0	0	0.6	0	0
V	0	0	0	0.6667	0
VI	0.1765	0.3529	0	0	0
VII	0.2727	0	0.2727	0	0
VIII	0	0.6667	0	-0.2222	0
IX	0.2	0.4	0	-0.1333	0
X	0.3333	0	0.3333	-0.2222	0
XII	0.3333	0	0	0.2222	0
XIII	0	0	1.	-0.6667	0
XV	0.2727	-0.5455	0	0	0.5455
	0.3529	-0.3529	0	0	0.3529
XVII	0.3333	-0.6667	-0.3333	0.2222	0.6667
	0.4	-0.4	-0.2	0.1333	0.4

TABLE XIII. FPs to the first order in ε for $m = 2$ and $n = 3$.

FP	u^*	v^*	w^*	y^*	z^*
I	0	0	0	0	0
II	0	0.6	0	0	0
III	0.4286	0	0	0	0
IV	0	0	0.5455	0	0
V	0	0	0	0.6667	0
VI	0.2727	0.2727	0	0	0
VII	0.1765	0	0.3529	0	0
VIII	0	1.	0	-0.6667	0
IX	0.3333	0.3333	0	-0.2222	0
X	0.2	0	0.4	-0.1333	0
XII	0.3333	0	0	0.2222	0
XIII	0	0	0.6667	-0.2222	0
XVI	0.2727	0	-0.5455	0	0.5455
	0.3529	0	-0.3529	0	0.3529
XVII	0.3333	-0.3333	-0.6667	0.2222	0.6667
	0.4	-0.2	-0.4	0.1333	0.4

$[0/2](\lambda)$. It is known that approximants from main diagonal of Padé-matrix⁸⁸ have best convergence properties, therefore in our calculations we use $[1/1](\lambda)$ approximant. Finally, the resummed β -function is found via inverse Borel transform:

$$\beta^{res}(u, v, w, y, z) = \int_0^\infty dt \exp(-t) [1/1](t). \quad (\text{C.4})$$

Applying this procedure for the analysis of the RG-functions (37)-(38e) (at the fixed dimension $d = 3$) and solving the corresponding system of non-linear FP equations, we obtain the sets of FPs for $m = 2$, $m = 3$ in the massive scheme as well as the $\overline{\text{MS}}$ scheme. Their coordinates are given in Tables III – VI.

TABLE XIV. FPs to the first order in ε for $m = 3$ and $n = 3$.

FP	u^*	v^*	w^*	y^*	z^*
I	0	0	0	0	0
II	0	0.5455	0	0	0
III	0.3529	0	0	0	0
IV	0	0	0.5455	0	0
V	0	0	0	0.6667	0
VI	0.0896	0.4478	0	0	0
VII	0.0896	0	0.4478	0	0
VIII	0	0.6667	0	-0.2222	0
IX	0.1053	0.5263	0	-0.1754	0
X	0.1053	0	0.5263	-0.1754	0
XII	0.2222	0	0	0.3704	0
XIII	0	0	0.6667	-0.2222	0

-
- ¹ A. Pelissetto and E. Vicari, Phys. Rept. **368**, 549 (2002).
² Vik. S. Dotsenko, Phys. Usp. **38**, 457 (1995); Usp. Fiz. Nauk **165**, 481 (1995).
³ Yu. Holovatch, V. Blavats'ka, M. Dudka, C. von Ferber, R. Folk, and T. Yavors'kii, Int. J. Mod. Phys. B, **16**, 4027 (2002).
⁴ R.B. Stinchcombe, in *Phase Transitions and Critical Phenomena*, edited by C. Domb and J. L. Lebowitz (Academic, London, 1983), Vol. 7, p. 152.
⁵ Y. Imry and S.K. Ma, Phys. Rev. Lett. **35**, 1399 (1975).
⁶ R. Harris, M. Plischke, and M.J. Zuckermann, Phys. Rev. Lett. **31**, 160, (1973).
⁷ R. Brout, Phys. Rev. **115**, 824-835 (1959).
⁸ A. B. Harris, J. Phys. C **7**, 1671 (1974).
⁹ R. Folk, Yu. Holovatch, and T. Yavors'kii Phys. Rev. B **61**, 15114 (2000).
¹⁰ A. Pelissetto and E. Vicari, Phys. Rev. B **62**, 6393 (2000).
¹¹ M. Tissier, D. Mouhanna, J. Vidal, and B. Delamotte, Phys. Rev. B **65**, 140402(R) (2002).
¹² A. Weinrib and B. I. Halperin, Phys. Rev. B **27**, 413 (1983).
¹³ E. R. Korutcheva, D. I. Uzunov, Phys. Status Solidi B **126**, K19 (1984).
¹⁴ E. Korutcheva and F. Javier de la Rubia, Phys. Rev. B **58**, 5153 (1998).
¹⁵ J. Honkonen and M. Y. Nalimov, J. Phys. A:Math. Gen. **22**, 751 (1989).
¹⁶ V. V. Prudnikov and A. A. Fedorenko, J. Phys. A **32**, L399 (1999).
¹⁷ V.V. Prudnikov, P.V. Prudnikov, and A.A. Fedorenko, Phys. Rev. B **62**, 8777 (2000).
¹⁸ M. Dudka, A. A. Fedorenko, V. Blavatska, and Yu. Holovatch, Phys. Rev. B **93**, 224422 (2016).
¹⁹ H. G. Ballesteros, G. Parisi, Phys. Rev. B **60**, 12912 (1999).
²⁰ D. Ivaneyko, B. Berche, Yu. Holovatch, and J. Ilnytskyi, Physica A **387**, 4497 (2008).
²¹ S.N. Dorogovtsev, Phys. Lett. **76A**, 169 (1980); Zh. Eksp. Teor. Fiz **80**, 2053 (1981) [Sov. Phys. JETP **53**, 1070 (1981)].
²² D. Boyanovsky and J.L. Cardy, Phys. Rev. B **26**, 154 (1982).
²³ V.V. Prudnikov, J. Phys. C **16**, 3685 (1983).
²⁴ I.D. Lawrie and V.V. Prudnikov, J. Phys. C **17**, 1655 (1984).
²⁵ Y. Yamazaki, A. Holz, M. Ochiai, and Y. Fukuda, Phys. Rev. B **33**, 3460 (1986); Y. Yamazaki, A. Holz, M. Ochiai, and Y. Fukuda, Physica A **150**, 576 (1988).
²⁶ V. Blavats'ka, C. von Ferber, and Yu. Holovatch, Phys. Rev. B **67**, 094404 (2003).
²⁷ L. De Cesare, Phys. Rev. B **49**, 11742 (1994).
²⁸ A.L. Korzhenevskii, A.A. Luzhkov, and W. Schirmacher, Phys. Rev. B **50**, 3661 (1994).
²⁹ A.A. Fedorenko, Phys. Rev. B **69**, 134301 (2004).
³⁰ V. Blavats'ka, M. Dudka, R. Folk, and Yu. Holovatch, Phys. Rev. B **72**, 064417 (2005); V. Blavats'ka, M. Dudka, R. Folk, and Yu. Holovatch, Journal of Molecular Liquids, **127**, 60 (2005);
³¹ O. Vasilyev, B. Berche, M. Dudka, and Yu. Holovatch, Phys. Rev. E **92**, 042118 (2015).
³² T. Nattermann, in *Spin Glasses and Random Fields*, edited by A.P. Young (World Scientific, Singapore, 1998), p.277.
³³ A. Aharony, Y. Imry and S.K. Ma, Phys. Rev. Lett. **37**, 1364 (1976); A.P. Young, J. Phys. C, **10**, L257 (1977).
³⁴ G. Tarjus and M. Tissier, Phys. Rev. Lett. **93**, 267008 (2004); M. Tissier and G. Tarjus, *ibid.* **96**, 087202 (2006).
³⁵ I. Balog, G. Tarjus, and M. Tissier, Phys. Rev. B **97**, 094204 (2018).
³⁶ G. Tarjus and M. Tissier, arXiv:1910.03530.
³⁷ D.E. Feldman, Phys. Rev. Lett. **84**, 4886 (2000); Phys. Rev. B **61**, 382 (2000); D. E. Feldman and R. A. Pelcovits, Phys. Rev. E **70**, 040702(R) (2004).
³⁸ D.E. Feldman, Phys. Rev. Lett. **88**, 177202 (2002).
³⁹ P. Le Doussal and K.J. Wiese, Phys. Rev. Lett. **96**, 197202, (2006).
⁴⁰ M. Tissier and G. Tarjus, Phys. Rev. B **74**, 214419 (2006).
⁴¹ A. A. Fedorenko and F. Kühnel, Phys. Rev. B **75**, 174206

- (2007).
- ⁴² A.A. Fedorenko, Phys. Rev. E **86**, 021131 (2012).
- ⁴³ A. Andreanov and A.A. Fedorenko Phys. Rev. B **90**, 014205 (2014).
- ⁴⁴ Y. Sakamoto, Phys. Rev. B **100**, 024412 (2019).
- ⁴⁵ R. W. Cochrane, R. Harris, and M. J. Zuckermann, Phys. Rep. **48**, 1 (1978).
- ⁴⁶ D.J. Sellmyer, M. J. O’Shea, in: D. H. Ryan (Ed.), Recent progress in random magnets, World Scientific, Singapore, (1992), p. 71.
- ⁴⁷ Y. Goldschmidt, in: D. H. Ryan (Ed.), Recent progress in random magnets, World Scientific, Singapore, (1992), p. 151.
- ⁴⁸ M. Dudka, Yu. Holovatch, and R. Folk, J. Magn. Magn. Mater. **294** 305 (2005).
- ⁴⁹ O.V. Billoni, S.A. Cannas, and F.A. Tamarit Phys. Rev. B **72**, 104407 (2005).
- ⁵⁰ D. Mouhanna and G. Tarjus, Phys. Rev. B **94**, 214205 (2016).
- ⁵¹ J. Zinn-Jutin, Quantum Field Theory and Critical Phenomena (Clarendon Press, Oxford, 1996).
- ⁵² D. J. Amit, Field Theory, the Renormalization Group, and Critical Phenomena (World Scientific, Singapore, 1989).
- ⁵³ H. Kleinert and V. Schulte-Frohlinde, *Critical Properties of ϕ^4 - Theories* - Singapore: World Scientific (2001).
- ⁵⁴ A. Aharony, Phys. Rev. B **12**, 1038 (1975).
- ⁵⁵ M. Dudka, R. Folk, and Yu. Holovatch, Condens. Matter Phys. **4**, 77 (2001).
- ⁵⁶ M. Dudka, Yu. Holovatch, R. Folk, in: W. Janke, A. Pelster, H.-J. Schmidt, M. Bachmann (Eds.), Fluctuating Paths and Fields, Singapore, World Scientific, p.457 (2001).
- ⁵⁷ M. Dudka, R. Folk, and Yu. Holovatch, Condens. Matter Phys. **4** 459 (2001).
- ⁵⁸ P. Calabrese, A. Pelissetto, and E. Vicari, Phys. Rev. E **70**, 036104 (2004) [[arXiv:cond-mat/0311576 v1](https://arxiv.org/abs/cond-mat/0311576)].
- ⁵⁹ D. Mukamel, G. Grinstein, Phys. Rev. B **25**, 381 (1982).
- ⁶⁰ V. Dubs, V. Prudnikov, and P. Prudnikov, Theoret. and Math. Phys., **190**, 359 (2017).
- ⁶¹ V. J. Emery, Phys. Rev. B **11**, 239-247 (1975)
- ⁶² K.H. Fisher and A. Zippelius, J. Phys. C: Solid State Phys. **18**, L1139 (1985); Prog. Theor. Phys. Suppl. **87**, 165 (1986).
- ⁶³ D. R. C. Dominguez and W. K. Theumann, Phys. Rev. B **48**, 6234 (1993).
- ⁶⁴ A.L. Korzhenevskii and A.A. Luzhkov, JETP **67** , 1229 (1988).
- ⁶⁵ J.C. Le Guillou and J. Zinn-Justin , Phys. Rev. B, **21**, 3976 (1980).
- ⁶⁶ R. Folk, Yu. Holovatch, and T. Yavors’kii, Physics-Uspekhi **46**, 169 (2003) [Uspekhi Fizicheskikh Nauk **173** 175 (2003)]; preprint [[cond-mat/0106468](https://arxiv.org/abs/cond-mat/0106468)].
- ⁶⁷ B. Delamotte, Yu. Holovatch, D. Ivaneyko, D. Mouhanna, and M. Tissier, J. Stat. Mech. (2008) P03014.
- ⁶⁸ B. Delamotte, M. Dudka, Yu. Holovatch, and D. Mouhanna, Phys. Rev. B **82**, 104432 (2010).
- ⁶⁹ B. Delamotte, M. Dudka, Yu. Holovatch, and D. Mouhanna, Condens. Matter Phys. **13**, 43703 (2010).
- ⁷⁰ B. Delamotte, M. Dudka, D. Mouhanna, S. Yabunaka, Phys. Rev. B **93**, 064405 (2016).
- ⁷¹ G. Parisi, Proceedings of the Cargr ese Summer School (1973) (unpublished); J. Stat. Phys **23**, 49-82 (1980).
- ⁷² G. ’t Hooft, Nucl. Phys. B. **44**, 189-213 (1972); *ibid* **61**, 455-468 (1973).
- ⁷³ B. Nickel, D. Meiron, G. Baker Jr., Univ. of Guelph Report (1977) (unpublished).
- ⁷⁴ Yu. Holovatch, T. Krokhmal’skii, J. Math. Phys. **35**, 3866 (1994); Yu. Holovatch and T. Yavors’kii, J. Stat. Phys. **92**, 785 (1998); Yu. Holovatch, M. Shpot, J. Stat. Phys. **66** (1992) 867.
- ⁷⁵ Aharony A. *Dependence of universal critical behaviour on symmetry and range of interaction*. in "Phase Transitions and Critical Phenomena", vol. 6, p. 357-424, edited by Domb C. and Green M.S. Academic, New York, (1976).
- ⁷⁶ M. Dudka, Yu. Holovatch, and T. Yavorskii, Acta Physica Slovaca, **52** 323 (2002); M. Dudka, Yu. Holovatch, and T. Yavors’kii, J. Phys. A, **37**, 10727 (2004).
- ⁷⁷ A. Stergiou, SciPost Phys. **7**, 010 (2019).
- ⁷⁸ L. Ts. Adzhemyan, E. V. Ivanova, M. V. Kompaniets, A. Kudlis, and A. I. Sokolov, Nucl. Phys. B, **940**, 332 (2019).
- ⁷⁹ S. R. Kousvos and A. Stergiou, SciPost Phys. **6**, 035 (2019).
- ⁸⁰ P. Calabrese, A. Pelissetto, and E. Vicari, Phys. Rev. B **67**, 024418 (2003).
- ⁸¹ R. Schloms and V. Dohm, Europhys. Lett. **3** 413 (1987); Nucl. Phys. B **328** 639 (1989).
- ⁸² D. Mukamel and S. Krinsky, Phys. Rev. B **13**, 5065 (1976).
- ⁸³ D.E. Khmel’nitskii, Zh. Eksp. Teor. Fiz. **68** 1960 (1975) [Sov. Phys. JETP **41** 981 (1975)]; A.B. Harris, T.C. Lubensky, Phys. Rev. Lett. **33** 1540 (1974); T.C. Lubensky, Phys. Rev. B **11** 3573 (1975); G. Grinstein, A. Luther, Phys. Rev. B **13** 1329 (1976).
- ⁸⁴ G. A. Baker, B. G. Nickel, M. S. Green, and D. Meiron, Phys. Rev. Lett. **36**, 1351 (1976); G. A. Baker, B. G. Nickel, and D. I. Meiron, Phys. Rev. B **17**, 1365 (1978).
- ⁸⁵ A.A. Berzin, A.I. Morosov, A.S. Sigov, Phys. Solid State **58**, 2018 (2016); A.A. Berzin, A.I. Morosov, A.S. Sigov, Phys. Solid State **59**, 2448 (2017); A.A. Berzin, A.I. Morosov, A.S. Sigov, J. Magn. Magn. Mater. **459**, 256 (2018).
- ⁸⁶ M. Abramowitz and I.A. Stegun, *Handbook of Mathematical Functions*, Dover (New York 1965).
- ⁸⁷ G. H. Hardy, *Divergent Series*, Oxford, (1948).
- ⁸⁸ G. Baker and P. Graves-Morris, *Pad e-Approximants*, Cambridge University Press, Cambridge, (1996).